

# Evaluation on the optical properties of $\text{Ga}_2\text{O}_3-x$ thin films co-doped with $\text{Tb}^{3+}$ and transition metals ( $\text{Mn}^{2+}$ , $\text{Cr}^{3+}$ ) prepared by a photochemical route

G. Cabello<sup>a,\*</sup>, L. Lillo<sup>a</sup>, C. Caro<sup>a</sup>, M.A. Soto-Arriaza<sup>b</sup>, B. Chornik<sup>c</sup>, G.E. Buono-Core<sup>d</sup>

<sup>a</sup>Departamento de Ciencias Básicas, Universidad del Bío-Bío, Avenida Andres Bello S/N, Campus Ferando May, Chillán, Chile

<sup>b</sup>Departamento Química-Física, Facultad de Química, Pontificia Universidad Católica de Chile, Casilla 306, Santiago 609441, Chile

<sup>c</sup>Departamento de Física, Facultad de Ciencias Físicas y Matemáticas, Universidad de Chile, Casilla 487-3, Santiago 8370415, Chile

<sup>d</sup>Instituto de Química, Pontificia Universidad Católica de Valparaíso, Valparaíso, Chile

Received 1 August 2012; accepted 31 August 2012

Available online 8 September 2012

## Abstract

Gallium  $\beta$ -diketonate complexes were studied as precursors for the photochemical deposition of amorphous thin films of gallium oxide doped with terbium and co-doped with chromium or manganese. Solutions of the inorganic complexes were spin coated on Si(100) and quartz substrates and photolyzed at room temperature using 254 nm UV light. The photolysis of these films induces the fragmentation of the complexes and the partial reduction of the metal ion together with the release of volatile organic compounds as sub-products. When the metallic complexes are irradiated under air, the products of the reactions are metal oxide thin films. The photochemical reactivity of these films was monitored by UV–vis spectroscopy, followed by a post-annealing treatment. The obtained films were characterized by X-ray photoelectron spectroscopy and X-ray diffraction. The optical properties of the films showed that these are highly transparent in the visible spectrum but decrease significantly in doped and co-doped films. Under UV light excitation (254 nm) the doped films ( $\text{Ga}_2\text{O}_3-x/\text{Tb}$ ) show the characteristic emissions at 486, 530, 542 and 610 nm associated to  $^5\text{D}_4 \rightarrow ^7\text{F}_J$  ( $J=6,5,4,3$ ) transitions of  $\text{Tb}^{3+}$  ion. However, these emissions decrease and deteriorate in the co-doped films ( $\text{Ga}_2\text{O}_3-x/\text{Tb}/\text{M}$ , where  $\text{M}=\text{Mn}$  or  $\text{Cr}$ ). A possible emission mechanism and energy transfer have been proposed.

© 2012 Elsevier Ltd and Techna Group S.r.l. All rights reserved.

**Keywords:** Photochemical deposition; Thin films; Optical materials; Luminescent materials

## 1. Introduction

Recently, lanthanide-doped luminescence materials have been intensively studied because of the potential applications in optoelectronic devices and flat panel displays [1]. For these applications, inorganic oxide materials known as phosphors, exhibit superior advantages in terms of their good chemical, thermal and mechanical properties [2]. Thus the  $\text{Ga}_2\text{O}_3$  exhibits different polymorphic phases such as rhombohedral  $\alpha$ , monoclinic  $\beta$ , cubic  $\gamma$  and  $\delta$  phases. Monoclinic gallium oxide ( $\beta\text{-Ga}_2\text{O}_3$ ) is a versatile oxide semiconductor material with a band gap of  $\sim 4.9$  eV, which exhibits particular conduction and luminescence properties [3]. Its wide band

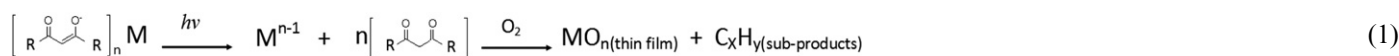
gap enables it to modify the luminescence properties by the incorporation of suitable ions in the  $\text{Ga}_2\text{O}_3$  lattice. In particular, doping  $\text{Ga}_2\text{O}_3$  with optically active ions, such as lanthanide (Ln) ions, allows for the synthesis of devices based on this material which can emit light at different wavelengths spanning from UV, all the way through the visible and the IR regions [4]. Numerous studies have reported on the properties of Ln ions doped  $\text{Ga}_2\text{O}_3$  as host material, such as  $\text{Ga}_2\text{O}_3\text{-Eu}$  [4–6],  $\text{Ga}_2\text{O}_3\text{-Tb}$  [1,7] and also the effect of some transition metals incorporated into  $\text{Ga}_2\text{O}_3$  as activators:  $\text{Ga}_2\text{O}_3\text{-Cr}$  [8,9]  $\text{Ga}_2\text{O}_3\text{-Mn}$  [8,10] are just some examples. The luminescence properties of inorganic compounds doped with various activators have been studied in recent years, specially the co-doping of ions in host materials, such as:  $\text{Eu}/\text{Tb}$  ions co-doped in  $\text{Ga}_2\text{O}_3$  nanoparticles obtained by solvothermal process [7],  $\text{Eu}/\text{Tb}$  ions co-doped in  $\text{SnO}_2$  films prepared by

\*Corresponding author. Tel.: +56 42 463096; fax: +56 42 463046.

E-mail address: [gcabello@ubiobio.cl](mailto:gcabello@ubiobio.cl) (G. Cabello).

sol–gel techniques [11], Er/Yb ions co-doped in GaN nanocrystalline powders [12] and Tb/Mn co-doped in glasses or glass ceramics [13].

The synthetic methods as well as the precursors are very important in obtaining material with the desired properties, especially relevant at nanometric scale. In this article we describe the use of the  $\beta$ -diketonate complexes of Ga(III), Tb(III), Mn(II) and Cr(III) to prepare films of gallium oxide doped with Tb and co-doped with transition metals such as Mn(II) and Cr(III). In this process the precursor complexes are spun onto a substrate forming an optical quality film. This film is then exposed to UV light resulting in the photo-extrusion of the ligands leaving the inorganic products on the surface. A general reaction is shown in Eq. (1). In this equation, the result of the photochemical reaction is the loss of the ligands from the metal center, generating a partial reduction of metal ion and further reaction with oxygen (in aerated conditions) resulting in the formation of metallic oxide thin film.



where R =  $-\text{CH}_3$  (acac) or  $-\text{C}(\text{CH}_3)_3$  (thd); M = Ga, Tb, Mn, Cr.

In this article, we report the results on the photo-deposition of gallium oxide thin films doped with Tb ( $\text{Ga}_2\text{O}_3-x/\text{Tb}$ ) and co-doped with Mn and Cr ( $\text{Ga}_2\text{O}_3-x/\text{Tb/M}$ ), and a preliminary study of their optical properties.

## 2. Experimental details

### 2.1. Preparation of amorphous thin films

The precursor Mn(II) and Cr(III) acetylacetonate complexes and Ga(III) and Tb(III) 2,2,6,6-tetramethyl-3,5-heptanedionate complexes were purchased from Aldrich Chemical Company and thin films were prepared by the following procedure: A silicon chip (n-type silicon (100) wafers ( $1 \times 1 \text{ cm}^2$ ) obtained from Wafer World Inc. Florida USA) was placed on a spin coater and rotated at a speed of 1500 rpm. A portion (0.1 ml) of a solution of the precursor complex in  $\text{CH}_2\text{Cl}_2$  was dispensed onto the silicon chip and allowed to spread. The motor was then stopped after 30 s and a thin film of the complex remained on the chip. The quality of the films was examined by optical microscopy ( $500 \times$  magnification).

### 2.2. Photolysis of complexes as films on Si (100) surfaces

All photolysis experiments were done following the same procedure: A film of the complex was deposited on n-type Si (100) by spin-coating from a  $\text{CH}_2\text{Cl}_2$  solution. This resulted in the formation of a smooth, uniform coating on the chip. The quality (uniformity, defects, etc.) of the precursor films was

examined by optical microscopy ( $500 \times$ ), while the thickness was monitored by optical interferometry (Leica DMLB optical microscope with Michelson interferometer). The FT-IR spectrum of the starting film was first obtained. The irradiation of the films was carried out at room temperature in air using two low-pressure Hg lamps (6 W, Rayonet RPR-2537 A), until the FT-IR spectrum showed no evidence of the starting material. Prior to analysis, the chip was rinsed several times with dry acetone to remove any organic products remaining on the surface. In order to obtain films of a specific thickness, successive layers of the precursors were deposited by spin-coating and irradiated as above. This process was repeated several times until the desired thickness was achieved. Post-annealing was carried out under a continuous flow of synthetic oxygen at  $850^\circ\text{C}$  for 3 h in a programmable Lindberg tube furnace.

### 2.3. Samples characterization

UV spectra were obtained with 1 nm resolution in a Perkin Elmer Model Lambda 25 UV–vis spectrophotometer. X-ray

diffraction patterns were obtained using a D8 Advance Bruker X-ray diffractometer. The X-ray source was Cu 40 kV/40 mA. X-ray photoelectron spectra (XPS) were recorded on an XPS-Auger Perkin Elmer electron spectrometer Model PHI 1257 which included an ultra high vacuum chamber, a hemispherical electron energy analyzer and an X-ray source providing unfiltered  $K\alpha$  radiation from its Al anode ( $h\nu = 1486.6 \text{ eV}$ ). The pressure of the main spectrometer chamber during data acquisition was maintained at ca  $10^{-7} \text{ Pa}$ . The binding energy (BE) scale was calibrated by using the peak of adventitious carbon, setting it to 284.6 eV. The accuracy of the BE scale was  $\pm 0.1 \text{ eV}$ .

Photoluminescence (PL) emission spectra measurements were carried out in an Ocean Optics Model QE65000-FL spectrometer with L type setup. Excitation was done with a PX-2 pulsed Xenon lamp (220–750 nm), and the UV light passed through a monochromator set to 254 nm. Time-resolved fluorescence measurements were performed on a K2 multifrequency phase and modulation spectrofluorometer (ISS, Champaign, IL, USA). The instrument was equipped with Glan-Thompson polarizers. Excitation light was obtained employing the modulable ISS 280 nm laser diode at frequencies between 0.009 and 0.09 MHz. The emission was measured through CG-455 long band-pass filters. Lifetime measurements were done with the polarizers oriented in the “magic angle” at  $54.7^\circ$  condition. In the multifrequency phase and modulation technique the intensity of the exciting light is modulated, and the phase shift and relative modulation of the emitted light are determined. Dimethyl-POPOP (1,4-bis[2]4-methyl-5-phenyloxazoly benzene) in ethanol ( $\tau = 1.45 \text{ ns}$ ) was used as a reference of intensity decay. In all measurements,

data were taken until the standard deviation of the phase and modulation measurements were, at each modulation frequency, smaller than  $0.2^\circ$  and  $0.004^\circ$ , respectively. The sample was placed at  $45^\circ$  respect to excitation light. The results were analyzed according to the Global Program (Global Unlimited software package, Laboratory for Fluorescence Dynamics, University of Illinois at Urbana-Champaign, Urbana, IL, USA).

### 3. Results and discussion

#### 3.1. Photochemistry of the precursor complexes

The photo-reactivity in solution of metal  $\beta$ -diketonate complexes has been extensively documented [14–16], as they absorb strongly at readily accessible portions of the UV spectrum (250–400 nm). In general terms, the photo-chemical reactivity, is initiated by the irradiation of a ligand-to-metal charge transfer (LMCT) band of the complex that causes the weakening and breaking of the metal–oxygen bond. This gives rise to the photo-reduction of the metal ion and the formation of radical species, depending on the nature of the complex and the photolysis conditions (nature of solvent, inert atmosphere or oxygenated atmosphere). In the literature no reports can be found concerning the photochemistry of  $\text{Ga}(\text{thd})_3$  and  $\text{Tb}(\text{thd})_3$  complexes. We therefore carried out experiments to evaluate the photosensitivity of these complexes in solution. When dichloromethane solutions of these complexes were photolyzed with 254 nm UV light, a rapid decrease in the absorption bands could be observed after 300 min (Fig. 1). These results demonstrated that both  $\beta$ -diketonate complexes are highly photo-reactive in solution when irradiated with 254 nm UV light.

#### 3.2. Characterization of $\text{Ga}_2\text{O}_{3-x}$ and $\text{Ga}_2\text{O}_{3-x}\text{-Tb/M}$ thin films (where $M = \text{Mn}$ or $\text{Cr}$ )

For the photo-deposition of thin films of gallium oxide doped with  $\text{Tb}(\text{III})$  and co-doped with  $\text{Mn}(\text{II})$  or  $\text{Cr}(\text{III})$ , solutions of  $\text{Ga}(\text{thd})_3$  with 10 mol% proportions of  $\text{Tb}(\text{thd})_3$

and with different proportions of the  $\text{M}(\text{acac})_3$  complexes (10, 5 and 1 mol%) were spin-coated on  $\text{Si}(100)$  or quartz substrates and the thin films irradiated for 24 h.

The elemental composition of as-deposited thin films was analyzed by XPS in order to investigate their chemical nature. Fig. 2 presents the XPS spectrum in the binding energy range of 0–1200 eV of undoped  $\text{Ga}_2\text{O}_3$  thin films photodeposited on a  $\text{Si}(100)$  surface. The spectrum shows signals from Ga 2p, Ga LMM (Auger peaks), O 1s, and C 1s. The carbon detected on the as-deposited films is probably the result of organic residues from the ligands. The amount of carbon was drastically reduced after mild  $\text{Ar}^+$  erosion, thus indicating that carbon is mainly deposited on the surface. As can be observed, energy peak for Ga 3d is centered at 19.8 eV, which is attributable to the presence of gallium oxide and not elemental gallium [17]. The Ga 3p peak at 105.6 eV confirmed the presence of  $\text{Ga}_2\text{O}_3$  which is consistent with other experimental results [18]. However, the most representative signals correspond to Ga 2p<sub>1/2</sub> and Ga 2p<sub>3/2</sub> located at 1145 and 1118 eV

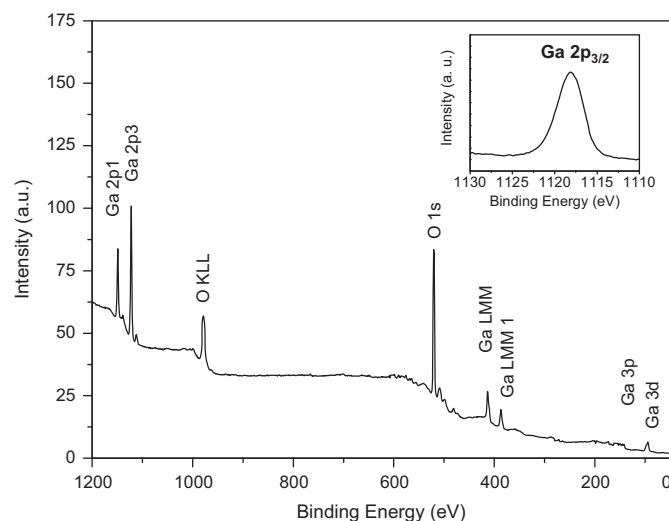


Fig. 2. XPS survey spectrum of an as-deposited un-doped  $\text{Ga}_2\text{O}_{3-x}$  thin film produced by UV irradiation of  $\text{Ga}(\text{thd})_3$  at 254 nm. Inset: Ga 2p<sub>3/2</sub> peak in the 1110–1130 eV region.

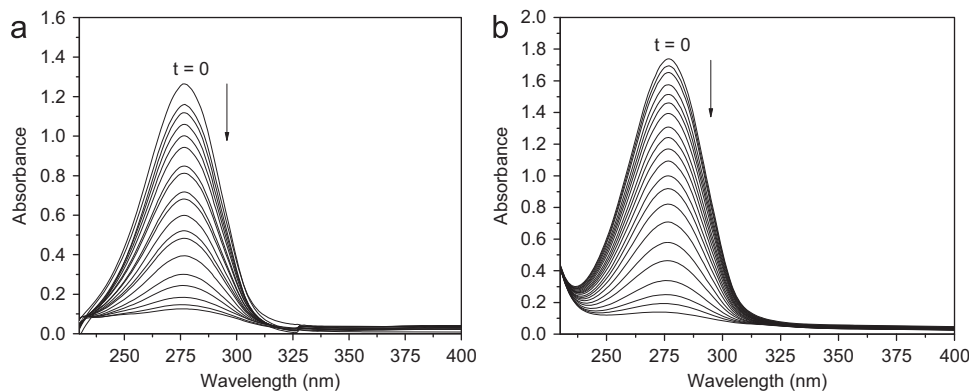


Fig. 1. Changes in the UV spectrum of a solution in  $\text{CH}_2\text{Cl}_2$  of (a)  $\text{Ga}(\text{thd})_3$  complex ( $4.1 \times 10^{-5}$  mol/L) upon 305 min irradiation and (b)  $\text{Tb}(\text{thd})_3$  complex ( $4.5 \times 10^{-5}$  mol/L) upon 195 min irradiation with 254 nm light.

respectively. The inset in Fig. 2 shows the XPS spectra of Ga  $2p_{3/2}$  at 1118 eV that confirms the presence of  $Ga_2O_3$  as reported by other authors [19]. The surface O 1s peak at 531.1 eV was found in the range expected for  $Ga_2O_3$  [18,19]. The weak tailing towards high binding energy could be due to the presence of adsorbed oxygen or hydroxyl species [18]. Upon erosion with  $Ar^+$ , the O 1s signal became narrower, thus indicating the almost complete disappearance of the high binding energy species in the sample layers. The quantification of peaks gives an atomic ratio of O/Ga close to 1.3, a lower value than that expected for stoichiometric  $Ga_2O_3$ , indicating that the as-deposited films are non-stoichiometric  $Ga_2O_{3-x}$ , where  $x$  is a small fraction.

The XPS spectra for thin films of  $Ga_2O_{3-x}$  co-doped with Tb/Mn and Tb/Cr are shown in Figs. 3 and 4 respectively. In both spectra, the Tb 4d signal can be fitted in two main sub-peaks, one centered at 148.1 eV assigned to the  $Tb^{3+}$  states and the other at 150.4 eV associated to the  $Tb^{4+}$  states. Similar values have been reported by other authors [20]. Other signals located at 1242.0 eV and 1276.1 eV have been attributed to photoemission peaks from Tb  $3d_{5/2}$  and Tb  $3d_{3/2}$  respectively [21]. A rigorous examination of the Tb  $3d_{5/2}$  peak reveals a broad peak very difficult to distinguish but appropriate fitting indicate that there are at least two chemical states ( $Tb^{3+}$  and  $Tb^{4+}$ ) [21].

A careful examination of the inset in Fig. 3 of Mn 2p levels shows two main peaks correspond to the spin-orbit split  $2p_{3/2}$  and  $2p_{1/2}$  levels [22]. The Mn  $2p_{3/2}$  level shows the presence of a strong overlap of the spectra implying the existence of Mn ions with different valence states. This signal can be fitted in three sub-peaks at 640.9, 642.4 and 646.1 eV corresponding to  $Mn^{2+}$ ,  $Mn^{4+}$  and  $Mn^{6+}$  species [23].

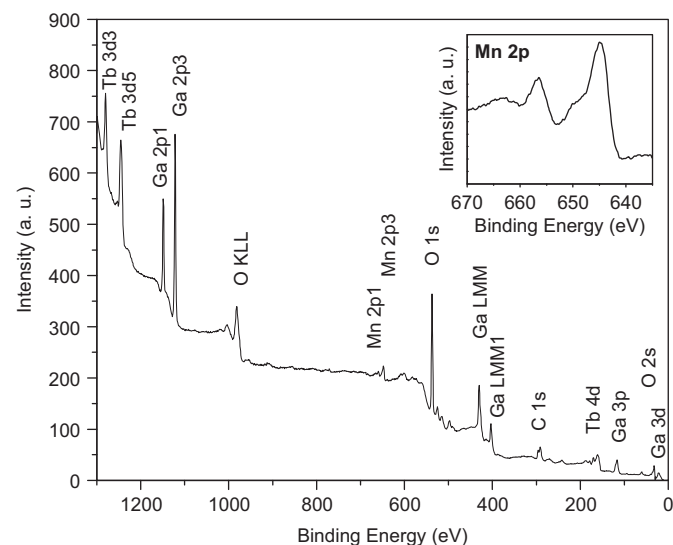


Fig. 3. XPS survey spectrum of an as-deposited  $Ga_2O_{3-x}$  thin film co-doped with Tb/Mn produced by UV irradiation at 254 nm. Inset: Mn 2p peaks in the 670–635 eV region.

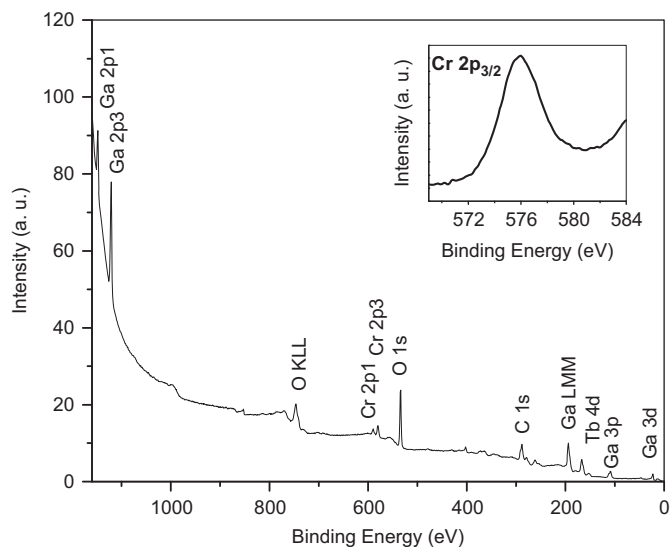


Fig. 4. XPS survey spectrum of an as-deposited  $Ga_2O_{3-x}$  thin film co-doped with Tb/Cr produced by UV irradiation at 254 nm. Inset: Cr  $2p_{3/2}$  peak in the 584–570 eV region.

On the other hand, the inset in Fig. 4 shows the XPS spectra of Cr  $2p_{3/2}$  peak for  $Ga_2O_{3-x}$  co-doped with Tb/Cr sample. This signal located at 576.3 eV can be attributable to Cr(III) species [23,24]. A comparison of these binding energy values with the standard values reported in literature [23,25] for different elements found in the samples are shown in Table 1.

In order to investigate the effect of thermal annealing on the structure of gallium oxide thin films, we have performed an XRD analysis on the samples annealed at 850 °C. XRD diffraction pattern of the annealed doped and co-doped  $Ga_2O_3$  films (not shown here) indicated the amorphous nature of the films, since no distinguishable  $Ga_2O_3$  diffraction peaks could be observed, except for the reflection from Si(100) located at  $2\theta=33.2^\circ$ . It has been reported that the use of  $\beta$ -diketonate complexes as precursors in the CVD process often result in amorphous films [18,26]. In fact, temperatures  $>900^\circ C$  are required to achieve some degree of crystallinity. The use of additional species such as  $O_2$  or  $O_3$  in the deposition processes may facilitate the formation of crystalline structures and also achieve the stoichiometry of the metallic oxides.

### 3.3. Optical properties

Fig. 5 showed the optical transmission spectra for undoped  $Ga_2O_{3-x}$ , doped  $Ga_2O_{3-x}-Tb^{3+}$  and co-doped  $Ga_2O_{3-x}-Tb^{3+}-M^{3+}$  thin films. Both, undoped  $Ga_2O_{3-x}$  and Tb doped  $Ga_2O_{3-x}$  films show a very high transmittance of more than 90% in the visible region. However for the  $Ga_2O_3$  co-doped films their transmittance spectra significantly decrease in the whole optical region. This indicates that the co-dopants are activated increasing the number of defects on the surface of film.

The optical band gaps of all samples are estimated by extrapolating the linear portion of the square of absorption

Table 1  
XPS results (binding energies, eV) for the photo-deposited samples.

Sample/signal	Ga 2p <sub>3/2</sub>	O 1s	Tb 3d <sub>5/2</sub>	Mn 2p <sub>3/2</sub>	Cr 2p <sub>3/2</sub>
Ga <sub>2</sub> O <sub>3-x</sub>	1118.0 ± 0.1	531.1 ± 0.1	–	–	–
Ga <sub>2</sub> O <sub>3-x</sub> /Tb/Mn	1118.1 ± 0.1	531.3 ± 0.1	1242.5 ± 0.1	640.9 ± 0.1 642.4 ± 0.1 646.1 ± 0.1	–
Ga <sub>2</sub> O <sub>3-x</sub> /Tb/Cr	1117.7 ± 0.1	530.8 ± 0.1	1242.0 ± 0.1	–	576.3 ± 0.1
Standard values at different oxidation states	1117.0 (Ga <sup>0</sup> ) 1118–1119 (Ga <sup>3+</sup> )	530–531 (O <sub>lat</sub> )* 532–535 (O <sub>ads</sub> )*	1239.4 (Tb <sup>0</sup> ) 1241–1242 (Tb <sup>3+</sup> ) 1241–1242 (Tb <sup>4+</sup> )	638.6 (Mn <sup>0</sup> ) 640.3 (Mn <sup>2+</sup> ) 641.2 (Mn <sup>3+</sup> ) 642–644 (Mn <sup>4+</sup> ) 645.5 (Mn <sup>6+</sup> )	574.2 (Cr <sup>0</sup> ) 575–577 (Cr <sup>3+</sup> ) 579.5 (Cr <sup>6+</sup> )

\*O<sub>lat</sub>)=attributed to lattice oxygen; (O<sub>ads</sub>)=attributed to chemisorbed oxygen on the metal surface.

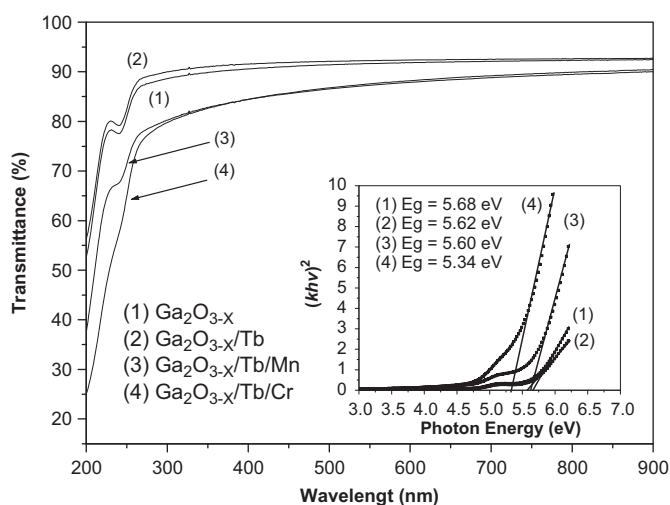


Fig. 5. Transmittance spectra of photo-deposited thin films of: (1) Ga<sub>2</sub>O<sub>3-x</sub>, (2) Ga<sub>2</sub>O<sub>3-x</sub> doped with Tb<sup>3+</sup>, (3) Ga<sub>2</sub>O<sub>3-x</sub> co-doped with 10 mol% of Tb/Mn and (4) Ga<sub>2</sub>O<sub>3-x</sub> co-doped with 10 mol% of Tb/Cr. Inset: Square of absorption coefficient as a function of photon energy.

coefficient against photon energy using the Eq. (2) where  $B$  is a constant.

$$(\alpha h\nu)^2 = B(h\nu - E_g) \quad (2)$$

The inset of Fig. 5 shows the plots of  $(\alpha h\nu)^2$  versus photon energy of the as-deposited un-doped, doped and co-doped Ga<sub>2</sub>O<sub>3-x</sub> films. The un-doped Ga<sub>2</sub>O<sub>3-x</sub> films have an optical band gap of 5.68 eV. This value is higher than those reported in other studies for un-doped Ga<sub>2</sub>O<sub>3</sub> that have established values of 4.8 [27] and 4.9 eV [28]. On the other hand, it has been reported that the  $\alpha$ -GaO(OH) phase has a  $E_g$  value of 5.27 eV [29] and for Ga<sub>2</sub>O<sub>3</sub> films deposited by pulsed spray pyrolysis a  $E_g$  value of 5.16 eV has been determined [30]. In our case we can attribute our value to the formation of non-stoichiometric Ga<sub>2</sub>O<sub>3-x</sub> thin films. The optical band gap of the Ga<sub>2</sub>O<sub>3-x</sub> doped and co-doped films varies between 5.62 and 5.34 eV. When a semiconductor lattice is doped by a foreign component with a much higher band gap, the incorporation between doped atoms and the lattice sites of the semiconductor will

increase the band gap of the semiconductor, which is the well-known band-gap engineering [31]. However, from previous studies, it can be concluded that the band gap value of gallium oxide strictly depends on its preparation conditions [32,33].

### 3.4. Photoluminescence study

Fig. 6 shows the photoluminescence (PL) spectra of gallium oxide doped and co-doped thin films under excitation at 254 nm. No signals can be observed for the un-doped gallium oxide thin film. However, films doped with 10 mol% of Tb (Ga<sub>2</sub>O<sub>3-x</sub>/Tb), show a series of bands at 486, 530, 542, 572 and 610 nm. These signals can be assigned to transitions from the excitation state <sup>5</sup>D<sub>4</sub> to the ground states <sup>7</sup>F<sub>*J*</sub> (*J*=6,5,4,3) of Tb ion in the host material [34,35]. On the other hand, for the co-doped films (Ga<sub>2</sub>O<sub>3-x</sub>/Tb/Mn and Ga<sub>2</sub>O<sub>3-x</sub>/Tb/Cr), it is possible to observe the same spectral pattern but their signal intensities decreased significantly. Moreover, there are no signals in the spectra that can be assigned to Mn and Cr ions. We have reported similar results in other studies [36]. In order to determine the co-doping of transition metal concentration dependence on the PL of the samples, the emission intensities were measured at concentration between 1 mol% and 10 mol% for Cr and Mn, and keeping the Tb concentration constant at 10 mol%. In Fig. 6 is shown the dependence of Cr (Fig. 6a) and Mn (Fig. 6b) concentration in the emission of all samples. The decrease observed in emission intensity with the increase of transition metal concentration is probably due to concentration-quenching effect [34].

On the other hand, the PL of samples annealed at 850 °C shows the same pattern of spectral behavior but their emission signals deteriorate and overlap (Fig. 7). It is known that local structural environments and spatial distribution of dopants and co-dopants are sensitive to their chemical and structural status in host material. In this case given the amorphous nature of the as-deposited and annealed films, there was no significant structural change to produce a noticeable change in the PL emissions. It has

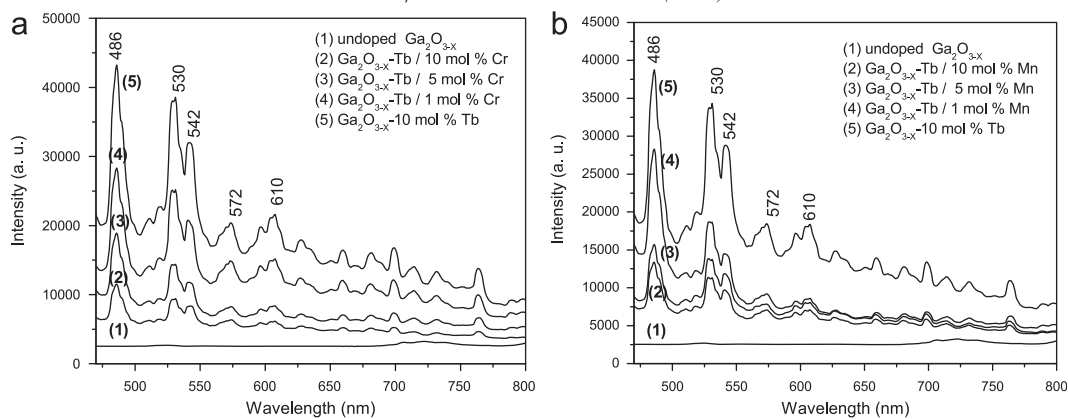


Fig. 6. PL spectra of as-deposited (a)  $\text{Ga}_2\text{O}_{3-x}/\text{Tb}/\text{Cr}$  and (b)  $\text{Ga}_2\text{O}_{3-x}/\text{Tb}/\text{Mn}$  thin films.

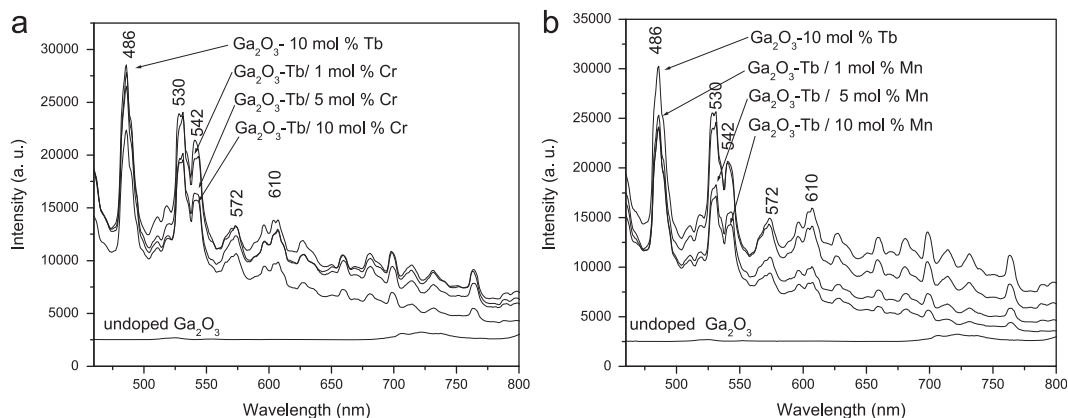


Fig. 7. PL spectra of (a)  $\text{Ga}_2\text{O}_{3-x}/\text{Tb}/\text{Cr}$  and (b)  $\text{Ga}_2\text{O}_{3-x}/\text{Tb}/\text{Mn}$  thin films, annealed at  $850^\circ\text{C}$ .

been reported [37] that the hydroxyl species or adsorbed oxygen in layered oxides could help to improve the energy transfer from layered oxide of host material to activator species rather than giving radiation less quenching via energy transfer to OH vibration like free water [38]. In this case these species on the surface of the films can act as bridge to enhance the interaction between the activators and the host material and thus improve the energy transfer process. However, further annealing of the samples at  $850^\circ\text{C}$  produces the loss of these species within the interlayer or surface of the films and therefore the emission intensities decrease significantly. In other studies [39] it is concluded that the photoluminescence properties of these materials are dependent on the hydration state by water molecules surrounding the activator in the interlayer or surface of the films. Therefore, the PL of Tb ions strongly depends on the chemical environment.

The lifetime values (Table 2) were obtained by excitation at 280 nm using a laser diode at frequencies between 0.009 and 0.09 MHz using 455 nm long band-pass filters. The measurement was carried out considering the following assumptions: (i) the homogeneous distribution of  $\text{Tb}^{3+}$  ions in the host matrix and (ii)  $\text{Tb}^{3+}$  ions may be located closer to the surface due to a strong matrix–activator interactions and a strong quenching effect at higher concentrations [34].

Table 2  
Lifetimes of the photo-deposited samples.

Sample	$\tau_1$ (ns)	$\chi^2$
$\text{Ga}_2\text{O}_{3-x}\text{-Tb}$	$11,300 \pm 45$	40,3
$\text{Ga}_2\text{O}_{3-x}\text{-Tb-Cr}$	$6570 \pm 60$	31,7
$\text{Ga}_2\text{O}_{3-x}\text{-Tb-Mn}$	$6355 \pm 120$	20,2

With respect of calculated emission lifetimes of  $\text{Tb}^{3+}$  ion, it is clear that the time emission of the  $\text{Ga}_2\text{O}_{3-x}\text{-Tb}$  films is significantly longer than that of the  $\text{Ga}_2\text{O}_{3-x}$  co-doped films. The decrease of emission decay rate in  $\text{Ga}_2\text{O}_{3-x}$ -co-doped films, can be attributed to the non-radiative process from Tb to transition metal of the co-doped films.

Although an energy transfer mechanism can be used to explain our results, it is important to mention the nature of defects centers in doped and co-doped gallium oxide and how they influence the optical properties. In this case, the excitation wavelength at 254 nm ( $\sim 4.8$  eV) is a lower energy than the band gap determined in most of our samples ( $> 5.0$  eV). The existence of oxygen vacancies generally act as deep defects donors in semiconductors and would cause the formation of new donor levels in the band gap. In the photo-excitation process, the electron from the valence band can be captured by donor level and then the

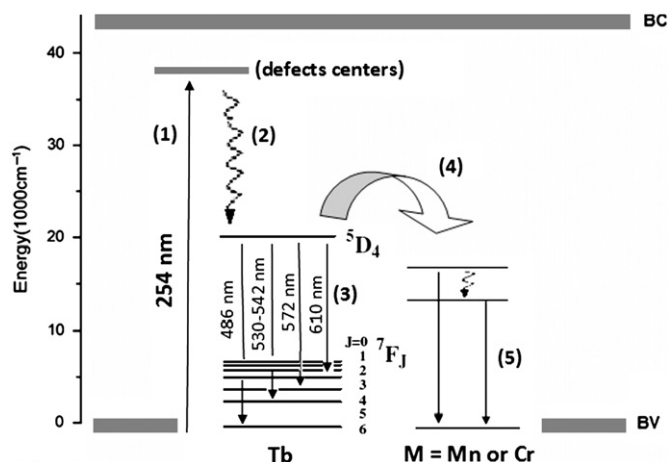


Fig. 8. Proposed mechanism for energy transfer and photoluminescence in  $\text{Ga}_2\text{O}_{3-x}\text{-Tb/M}$  thin films (where  $M=\text{Mn}$  or  $\text{Cr}$ ).

energy transfer to lanthanide ion allows for the emission processes. However, if the energy levels of these defects are lower than the energy levels of the lanthanide ion, the energy transfer process does not occur and consequently the PL emission cannot be observed. Given that the excited state energy level of terbium ion ( $^5\text{D}_4$ ) is approximately 2.55 eV, this energy value is lower than the energy levels of defects of material host. Thus the energy level of gallium oxide defects is not below this value.

In order to explain our PL results, we propose a qualitative model for the absorption, energy transfer and radiative relaxation, using a similar model proposed by other authors [40]. The mechanism proposed (Fig. 8) consists of (1) Absorption of light (254 nm) and excitation from valence band to defects centers of  $\text{Ga}_2\text{O}_{3-x}$  located near the conduction band (induced by oxygen vacancies); (2) non-radiative energy transfer process from defects centers to  $^5\text{D}_4$  excited state level of Tb ion; (3) radiative energy process from the excited state  $^5\text{D}_4$  to the ground levels of  $^7\text{F}_J$  ( $J=6,5,4,3$ ) of Tb ion; (4) non-radiative energy transfer from the excited state  $^5\text{D}_4$  to the defects caused by co-doping of Mn or Cr leading to the decrease in emission intensity of samples. This decrease is more significant with increasing concentration of transition metal; and (5) non-radiative relaxation process of transition metal.

#### 4. Conclusions

The  $\text{Ga}_2\text{O}_{3-x}\text{-Tb}$  and  $\text{Ga}_2\text{O}_{3-x}\text{-Tb/M}$  thin films (where  $M=\text{Mn}$  or  $\text{Cr}$ ), were prepared by a simple photochemical method, using  $\beta$ -diketonate complexes as precursors. The compositional and structural characterization of the films using XPS and XRD, respectively, revealed the formation of  $\text{Ga}_2\text{O}_{3-x}$  as host material, Tb as activator and Mn and Cr as co-dopants. The amorphous characteristics of the films strongly determine the non-crystalline nature of the as-photo-deposited samples and their photo-luminescent properties. Under excitation at 254 nm the doped films show the characteristic emissions associated to  $^5\text{D}_4 \rightarrow ^7\text{F}_J$

( $J=6,5,4,3$ ) transitions of Tb ion, but these emissions decrease and deteriorate with co-doping and annealing of the films. Nevertheless, more investigation is required in order to study the influence of the defects and of the annealing temperature on the PL properties of photo-deposited thin films.

#### Acknowledgments

The authors are grateful for the financial support of FONDECYT (National Fund for Scientific and Technological Development), Chile, Grant no. 1100045.

#### References

- [1] J. Zhao, W. Zhang, E. Xie, Z. Liu, J. Feng, Z. Liu, Photoluminescence properties of  $\beta\text{-Ga}_2\text{O}_3\text{:Tb}^{3+}$  nanofibers prepared by electrospinning, *Materials Science and Engineering B* 176 (2011) 932–936.
- [2] H. Yang, R. Shi, J. Yu, R. Liu, R. Zhang, H. Zhao, L. Zhang, H. Zheng, Single-crystalline  $\beta\text{-Ga}_2\text{O}_3$  hexagonal nanodisks: synthesis, growth mechanism, and photocatalytic activities, *Journal of Physical Chemistry C* 113 (2009) 21548–21554.
- [3] Kh.M. Al-khamis, R.M. Mahfouz, A.A. Al-warthan, M.R. Siddiqui, Synthesis and characterization of gallium oxide nanoparticles, *Arabian Journal of Chemistry* 2 (2009) 73–77.
- [4] J. Zhao, W. Zhang, E. Xie, Z. Ma, A. Zhao, Z. Liu, Structure and photoluminescence of  $\beta\text{-Ga}_2\text{O}_3\text{:Eu}^{3+}$  nanofibers prepared by electrospinning, *Applied Surface Science* 257 (2011) 4968–4972.
- [5] H. Xie, L. Chen, Y. Liu, K. Huang, Preparation and photoluminescence properties of Eu-doped  $\alpha$ - and  $\beta\text{-Ga}_2\text{O}_3$  phosphors, *Solid State Communications* 141 (2007) 12–16.
- [6] J.S. Kim, H.E. Kim, H.L. Park, G.C. Kim, Luminescence intensity and color purity enhancement in nanostructured  $\beta\text{-Ga}_2\text{O}_3\text{:Eu}^{3+}$  phosphors, *Solid State Communications* 132 (2004) 459–463.
- [7] G. Sinha, A. Patra, Generation of green, red and white light from rare-earth doped  $\text{Ga}_2\text{O}_3$  nanoparticles, *Chemical Physics Letters* 473 (2009) 151–154.
- [8] T. Miyata, T. Nakatani, T. Minami, Gallium oxide as host material for multicolor emitting phosphors, *Journal of Luminescence* 87–89 (2000) 1183–1185.
- [9] S. Fujihara, Y. Shibata, Luminescence of  $\text{Cr}^{3+}$  ions associated with surpassing the green-emissive defect centers in  $\beta\text{-Ga}_2\text{O}_3$ , *Journal of Luminescence* 121 (2006) 470–474.
- [10] T. Miyata, T. Nakatani, T. Minami, Manganese-activated gallium oxide electroluminescent phosphor thin films prepared using various deposition methods, *Thin Solid Films* 373 (2000) 145–149.
- [11] H. Elhouichet, A. Moadhen, M. Ferid, M. Ouslati, B. Canut, J.A. Roger, High luminescent  $\text{Eu}^{3+}$  and  $\text{Tb}^{3+}$  doped  $\text{SnO}_2$  sol-gel derived films deposited on porous silicon, *Physica Status Solidi A* 197 (2003) 350–354.
- [12] M. Nyk, A. Kuzmin, P.N. Prasad, W. Strek, Cid B. de Araujo, Red up-conversion emission from nanocrystalline GaN powders co-doped with  $\text{Er}^{3+}$  and  $\text{Yb}^{3+}$ , *Optical Materials* 31 (2009) 800–804.
- [13] Y. Liu, Z. Zou, X. Liang, S. Wang, Z. Xing, G. Chen, Energy transfer and photoluminescence of zinc phosphate glasses co-doped with  $\text{Tb}^{3+}$  and  $\text{Mn}^{2+}$ , *Journal of the American Ceramic Society* 93 (2010) 1891–1893.
- [14] B. Marciniak, G.E. Buono-Core, Photochemical properties of 1,3-diketonate transition metal chelates, *Journal of Photochemistry and Photobiology A: Chemistry* 52 (1990) 1–25.
- [15] S. Giuffrida, G.G. Condorelli, L.L. Costanzo, I.L. Fragala, G. Ventimiglia, G. Vecchio, Photochemical mechanism of the formation of nanometer-sized copper by UV irradiation of ethanol bis(2,4-pentandionato)copper(II) solutions, *Chemistry of Materials* 16 (2004) 1260–1266.

- [16] S. Giuffrida, L.L. Costanzo, G.G. Condorelli, G. Ventimiglia, I.L. Fragala, Photochemistry of bis(1,1,1,5,5,5-hexafluoro-2,4-pentanedionato)strontium tetraglyme solutions for eventual liquid phase photochemical deposition, *Inorganica Chimica Acta* 358 (2005) 1873–1881.
- [17] Q. Xu, S. Zhang, Fabrication and photoluminescence of  $\beta$ -Ga<sub>2</sub>O<sub>3</sub> nanorods, Superlattices and Microstructures 44 (2008) 715–720.
- [18] M. Hellwig, Ke Xu, D. Barreca, A. Gasporotto, M. Winter, E. Tondello, R. Fischer, A. Devi, Novel gallium complexes with malonic diester anions as molecular precursors for the MOCVD of Ga<sub>2</sub>O<sub>3</sub> thin films, *European Journal of Inorganic Chemistry* 8 (2009) 1110–1117.
- [19] A. Trinchì, S. Kaciulis, L. Pandolfi, M.K. Ghantasala, Y.X. Li, W. Wlodarski, S. Viticoli, E. Comini, G. Sberveglieri, Characterization of Ga<sub>2</sub>O<sub>3</sub> based MRISiC hydrogen gas sensors, *Sensors and Actuators B* 103 (2004) 129–135.
- [20] D. Lonappan, N.V. Chandra Shekar, P.Ch. Sahu, J. Kumar, R. Paul, P. Paul, Unusually large structural stability of terbium oxide phase under high pressure, *Journal of Alloys and Compounds* 490 (2010) 47–49.
- [21] A. Martínez-Arias, A.B. Hungria, M. Fernández-García, A. Iglesias-Juez, J.C. Conesa, G.C. Mather, G. Munuera, Cerium–terbium mixed oxides as potential materials for anodes in solid oxide fuel cells, *Journal of Power Sources* 151 (2005) 43–51.
- [22] G. Zampieri, M. Abbate, F. Prado, A. Caneiro, Mn-2p XPS spectra of differently hole-doped Mn perovskites, *Solid State Communications* 123 (2002) 81–85.
- [23] M. Biesinger, B. Payne, A. Grosvenor, L. Lau, A. Gerson, R. Smart, Resolving surface chemical states in XPS analysis of first row transition metals, oxides and hydroxides: Cr, Mn, Fe, Co and Ni, *Applied Surface Science* 257 (2011) 2717–2730.
- [24] M.F. Al-Kuhaili, S.M.A. Durrani, Optical properties of chromium oxide thin films deposited by electron-beam evaporation, *Optical Materials* 29 (2007) 709–713.
- [25] C.D. Wagner, A.V. Naumkin, A. Kraut-Vass, J.W. Allison, C.J. Powell, J.R. Rumble, NIST Standard Reference Database 20, Version 3.5, 2003. <<http://srdata.nist.gov/xps/>>.
- [26] M. Leskela, K. Kukli, M. Ritala, Rare-earth oxide thin films for gate dielectrics in microelectronics, *Journal of Alloys and Compounds* 418 (2006) 27–34.
- [27] Y. Zhang, J. Yan, Q. Li, C. Qu, L. Zhang, W. Xie, Optical and structural properties of Cu-doped  $\beta$ -Ga<sub>2</sub>O<sub>3</sub> films, *Materials Science and Engineering B* 176 (2011) 846–849.
- [28] G. Sinha, K. Adhikary, S. Chaudhuri, Sol–gel derived phase pure  $\alpha$ -Ga<sub>2</sub>O<sub>3</sub> nanocrystalline thin film and its optical properties, *Journal of Crystal Growth* 276 (2005) 204–207.
- [29] G. Sinha, K. Adhikary, S. Chaudhuri, Effect of annealing temperature on structural transformation of gallium based nanocrystalline oxide thin films and their optical properties, *Optical Materials* 29 (2007) 718–722.
- [30] Z. Ji, J. Du, J. Fan, W. Wang, Gallium oxide films for filter and solar-blind UV detector, *Optical Materials* 28 (2006) 415–417.
- [31] L. Xu, B. Dong, Y. Wang, X. Bai, J. Chen, Q. Liu, H. Song, Porous In<sub>2</sub>O<sub>3</sub>:RE (RE=Gd, Tb, Dy, Ho, Er, Tm, Yb) nanotubes: electrospinning preparation and room gas-sensing properties, *Journal of Physical Chemistry C* 114 (2010) 9089–9095.
- [32] G. Sinha, D. Ganguli, S. Chaudhuri, Crystallization and optical properties of finite sized  $\beta$ -Ga<sub>2</sub>O<sub>3</sub> in sol–gel derived Ga<sub>2</sub>O<sub>3</sub>:SiO<sub>2</sub> nanocomposites, *Journal of Physics Condensed Matter* 18 (2006) 11167.
- [33] G. Cabello, L. Lillo, C. Caro, G.E. Buono-Core, B. Chornik, M.A. Soto, Structure and optical characterization of photochemically prepared ZrO<sub>2</sub> thin films doped with erbium and europium, *Journal of Non-Crystalline Solids* 354 (2008) 3919.
- [34] N. Yaiphaba, R.S. Ningthoujan, N.R. Singh, R.K. Vatsa, Luminescence properties of redispersible Tb<sup>3+</sup>-doped GdPO<sub>4</sub> nanoparticles prepared by an ethylene glycol route, *European Journal of Inorganic Chemistry* 18 (2010) 2682–2687.
- [35] G. Chen, Y. Yang, D. Zhao, F. Xia, Composition effects on optical properties of Tb<sup>3+</sup>-doped heavy germanate glasses, *Journal of the American Ceramic Society* 88 (2005) 293–296.41.
- [36] G. Cabello, L. Lillo, Y. Huentupil, F. Cabrera, G.E. Buono-Core, B. Chornik, A simple photochemical method to synthesize Ga<sub>2</sub>O<sub>3</sub>–Dy<sup>3+</sup>–M<sup>3+</sup> thin films and their evaluation as optical materials (where M=Cr or Co), *Journal of Physics and Chemistry of Solids* 72 (2011) 1170–1174.
- [37] J. Yin, X. Zhao, Facile synthesis and the sensitized luminescence of europium ions-doped titanate nanowires, *Materials Chemistry and Physics* 114 (2009) 561–568.
- [38] Y. Matsumoto, U. Unal, Y. Kimura, S. Ohashi, K. Izawa, Synthesis and photoluminescent properties of titanate layered oxides intercalated with lanthanide cations by electrostatic self-assembly methods, *Journal of Physics Chemistry B* 109 (2005) 12748–12754.
- [39] S. Ida, U. Unal, K. Izawa, O. Altuntasoglu, C. Ogata, T. Inoue, K. Shimogawa, Y. Matsumoto, Photoluminescence spectral change in layered titanate oxide intercalated with hydrated Eu<sup>3+</sup>, *Journal of Physical Chemistry B* 110 (2006) 23881–23887.
- [40] L. Hu, H. Song, G. Pan, B. Yan, R. Qin, Q. Dai, L. Fan, S. Li, X. Bai, Photoluminescence properties of samarium-doped TiO<sub>2</sub> semiconductor nanocrystalline powders, *Journal of Luminescence* 127 (2007) 371–376.